Oropouche virus glycoprotein topology and cellular requirements for virus assembly

Natalia S. Barbosa[a,b,c], Juan O. Concha[a,b], Luis L. P. daSilva[a,b], Colin M. Crump[c#], Stephen C. Graham[c#]

[a] Center for Virus Research, Ribeirão Preto Medical School, University of São Paulo, Ribeirão Preto, SP, Brazil

[b] Department of Cell and Molecular Biology, Ribeirão Preto Medical School, University of São Paulo, Ribeirão Preto, SP, Brazil

[c] Department of Pathology, University of Cambridge, Cambridge, United Kingdom

[#] Address correspondence to Colin M. Crump, cmc56@cam.ac.uk, or Stephen C. Graham, scg34@cam.ac.uk.

ORCIDs: 0000-0002-2926-5294 (NSB), 0000-0003-3257-2348 (JOC), 0000-0003-3558-0087 (LLPdS), 0000-0001-9918-9998 (CMC), 0000-0003-4547-4034 (SCG)

Running title: Determinants of Oropouche virus glycoprotein release

Keywords: Bunyavirus, Bunyamwera virus, polyprotein processing, virus budding

Author Contributions: Conceptualization: LLPdS, CMC, SCG; Funding Acquision: NSB, LLPdS, CMC, SCG; Investigation: JOC, NSB; Methodology: LLPdS, CMC, SCG; Resources: LLPdS, CMC, SCG; Supervision: LLPdS, CMC, SCG; Visualization: NSB, SCG; Writing – original draft: NSB, SCG; Writing – review & editing: NSB, LLPdS, CMC, SCG.

Abstract

Oropouche virus (OROV; *Genus: Orthobunyavirus*) is the etiological agent of Oropouche fever, a debilitating febrile illness common in South America. We used recombinant expression of the OROV M polyprotein, that encodes the surface glycoproteins Gn and Gc plus the non-structural protein NSm, to probe the cellular determinants for OROV assembly and budding. Gn and Gc self-assemble and are secreted independently of NSm. Mature OROV Gn has two predicted transmembrane domains that are crucial for glycoprotein translocation to the Golgi complex and glycoprotein secretion and, unlike related orthobunyaviruses, both transmembrane domains are retained during Gn maturation. Disruption of Golgi function using the drugs brefeldin A and monensin inhibit glycoprotein secretion. Infection studies have previously shown that the cellular Endosomal Sorting Complexes Required for Transport (ESCRT) machinery is recruited to Golgi membranes during OROV assembly and that ESCRT activity is required for virus secretion. A dominant negative form of the ESCRT-associated ATPase VPS4 significantly reduces recombinant OROV glycoprotein secretion and blocks virus release from infected cells, and VPS4 partly co-localizes with OROV glycoproteins and membranes co-stained with Golgi markers. Furthermore, immunoprecipitation and fluorescence microscopy experiments demonstrate that OROV glycoproteins interact with the ESCRT-III component CHMP6, with overexpression of a dominant negative form of CHMP6 significantly reducing OROV glycoprotein secretion. Taken together, our data highlights differences in M polyprotein processing across orthobunyaviruses, that Golgi and ESCRT function are required for glycoprotein secretion, and identifies CHMP6 as an ESCRT-III component that interacts with OROV glycoproteins.

Importance

Oropouche virus causes Oropouche fever, a debilitating illness common in South America that is characterised by high fever, headache, myalgia and vomiting. The tripartite genome of this zoonotic virus is capable of reassortment and there have been multiple epidemics of Oropouche fever in South America over the last 50 years, making Oropouche virus infection a significant threat to public health. However, the molecular characteristics of this arbovirus are poorly understood. We developed a recombinant protein expression system to investigate the cellular determinants of OROV glycoprotein maturation and secretion. We show that the proteolytic processing of the M polypeptide, which encodes the surface glycoproteins (Gn and Gc) plus a non-structural protein (NSm), differs between OROV and its close relative Bunyamwera virus. Furthermore, we demonstrate that OROV M glycoprotein secretion requires the cellular ESCRT membrane-remodelling machinery and identify that the OROV glycoproteins interact with the ESCRT protein CHMP6.

53 **Introduction**

54 Oropouche virus (OROV) is an arbovirus that is the etiological agent of Oropouche fever, a debilitating
55 febrile illness. Oropouche fever symptoms range from high fever to vomiting, photophobia and, in rare
56 cases, aseptic meningitis or meningoencephalitis (1). OROV is prevalent in the Caribbean and tropical
57 regions of Latin America, and more than 30 epidemics of Oropouche fever have occurred since the first
58 isolation of OROV in 1955 (1). Clinical diagnosis of Oropouche fever is challenging due to the
59 resemblance of its symptoms to diseases caused by other arboviruses like Dengue virus, Zika virus
60 and Chikungunya virus (2). There are no specific antiviral treatments for Oropouche fever, nor is there
61 an effective vaccine to prevent OROV infection. The zoonotic origin, history of human spill-over, tri-
62 segmented RNA genome that is capable of re-assortment (3) and increasing contact between humans
63 and wild-animal reservoirs due to deforestation (1) make OROV a serious epidemic threat.

64 OROV belongs to *Orthobunyavirus* genus of the *Peribunyaviridae* family, one of the fourteen families
65 of the order *Bunyavirales*. Orthobunyaviruses form spherical enveloped virus particles that are 100–
66 120 nm in diameter and orthobunyavirus genomes comprise three negative sense single-stranded RNA
67 segments: The small segment (S) encodes the nucleocapsid N protein (25–30 kDa), which oligomerizes
68 and encapsidates the viral genome, and the non-structural protein NSs; The medium segment (M)
69 encodes a polyprotein that is co-translationally cleaved by host proteases to yield the viral surface
70 glycoproteins (Gc and Gn) plus a non-structural protein NSm; The large segment (L) encodes the viral
71 RNA dependent RNA polymerase (RdRp) that catalyzes viral replication and transcription (4). The viral
72 RNA segments are encapsidated by N protein to form a ribonucleoprotein complex that associates with
73 both the RdRp and the surface glycoproteins to promote virus particle assembly (5). The Gn (~32 kDa)
74 and Gc (~110 kDa) glycoproteins are integral membrane proteins with N-terminal ectodomains and they
75 associate in the host endoplasmic reticulum (ER) before being transported to the Golgi complex, the
76 main site of virion assembly (6–8). Studies with Bunyamwera virus (BUNV), the prototypical
77 orthobunyavirus, have shown that the virus particles undergo distinct morphological changes inside
78 Golgi and *trans*-Golgi network cisternae (7), and studies of both BUNV and OROV have shown profound
79 fragmentation on Golgi complex cisternae during virus infection of some cell types (6, 7).

80 OROV assembly at the Golgi complex is stimulated by the cellular Endosomal Sorting Complexes
81 Required for Transport (ESCRT) machinery (6). The ESCRT machinery is most commonly associated
82 with membrane deformation and scission in an 'inside-out' topology, in contrast to the 'outside-in'
83 topology of endocytic vesicles (9). The human ESCRT machinery comprises multiple distinct protein
84 complexes (ESCRT-0, ESCRT-I, ESCRT-II and ESCRT-III) plus several accessory proteins, with final
85 membrane scission being promoted by the concerted action of ESCRT-III and the ATPase VPS4 (10).
86 The ESCRT-III machinery is formed by members of the charged multivesicular body protein (CHMP)
87 family, with distinct CHMP proteins playing specific coordinated roles. The first ESCRT-III component
88 recruited is CHMP6, which recruits CHMP4 isotypes (CHMP4A or CHMP4B) to homo-oligomerizes at
89 the target membrane. The CHMP2A plus CHMP3 complex and/or CHMP2B alone are then recruited,
90 activating VPS4 to promote ESCRT-III filament disassembly and membrane scission (10–12). Virus

91 recruitment of the ESCRT-III machinery is canonically mediated by direct association of viral 'late
92 domains' with ESCRT-I, the cellular ubiquitylation machinery and/or the accessory protein ALIX. These
93 interactions culminate in recruitment and activation of the ESCRT-III machinery (13, 14). With the
94 exception of flaviviruses, which recruit ESCRT components to the ER (15), most viruses recruit ESCRT
95 machinery to the plasma membrane, endosomes or other 'post-Golgi' membranes (14, 16). It is
96 therefore particularly interesting that OROV budding involves direct recruitment of ESCRT machinery
97 to Golgi membranes (6). The OROV glycoproteins do not contain any identifiable viral 'late domains'
98 and the molecular basis of ESCRT machinery recruitment by OROV thus remains to be established.

99 The study of many orthobunyaviruses requires high-level biosafety containment, owing to their ability
100 to cause severe human disease and a lack of effective vaccines. Recombinant systems that recapitulate
101 key aspects of virus biology are thus desirable to facilitate investigation under reduced biosafety
102 containment of the assembly pathways of these highly-pathogenic virus (17, 18). Plasmid-based
103 recombinant virus-like particle (VLP) production systems have been established for several members
104 of the order *Bunyavirales*, with phlebovirus and hantavirus VLP assembly requiring expression of the
105 viral glycoproteins but not the nucleoprotein (19, 20). Mini-replicon systems where the M polyprotein, L
106 protein (RdRP) and nucleoprotein are recombinantly expressed on plasmids to generate VLPs has
107 been reported for several orthobunyaviruses including BUNV, OROV, La Crosse virus (LACV),
108 Akabane virus, and Schmallenberg virus (SBV) (21–27). Additionally, transcription- and replication-
109 competent VLPs facilitate measurement of subtle differences in LACV and Rift Valley fever virus
110 (RVFV) RdRp activity (27). Given that OROV recombinant virus lacking NSm is fully infectious (28) and
111 that the signal peptide of NSm (SP^{NSm}) is cleaved from the BUNV Gn protein during virion maturation
112 (29), we hypothesised that recombinantly expressed OROV glycoproteins Gn and Gc would self-
113 associate and be release from cells in a VLP-like manner.

114 Here we report OROV glycoprotein secretion via recombinant expression of the M polyprotein. The
115 mature OROV Gn protein appears to contain two transmembrane domains (TMDs), both when
116 expressed recombinantly and in the context of infection, and the second TMD is crucial for glycoprotein
117 delivery to the Golgi and subsequent secretion. Pharmacological disruption of Golgi function prevents
118 OROV glycoprotein secretion, as does perturbation of ESCRT function, highlighting the utility of this
119 secretion assay for probing cellular determinants of OROV assembly. Finally, we show that the ESCRT-
120 III component CHMP6 interacts with the OROV glycoproteins, suggesting that interaction between
121 OROV glycoproteins and CHMP6 may facilitate OROV assembly and release.

122

Results

Processing and secretion of recombinant OROV glycoproteins

A synthetic codon-optimised cDNA encoding the OROV medium (M) segment polyprotein (residues 1–1420) was cloned into the mammalian expression vector pcDNA3.1 with an HA epitope tag between the secretion signal sequence (SS; residues 1–16) and the first residue of the mature Gn protein (Fig. 1A). Transfection of HEK293T cells with a plasmid encoding HA-tagged OROV M polyprotein yielded high levels of Gn and Gc (observed as bands at ~35 kDa and ~120 kDa, respectively) in the supernatant, confirming secretion of OROV glycoproteins by these transfected cells (Fig. 1B). In order to establish whether both OROV glycoproteins are required for secretion, OROV Gn (M polyprotein residues 17–313) and Gc (M polyprotein residues 482–1420) were cloned separately into pcDNA3.1 after the OROV M SS and HA epitope tag (Fig. 1A), the polyprotein cleavage sites being inferred from homology with those determined or predicted for the BUNV M polyprotein (29). Domain boundaries were chosen based on prior studies of OROV and BUNV glycoproteins (29, 30) and analysis of predicted TMD topology (31). As expected, neither Gn nor Gc was abundant in the cell supernatant when transfected into HEK293T cells in isolation. However, we also failed to observe secreted glycoproteins when the proteins were co-expressed (Fig. 1B). This was unexpected as a previous study of OROV infection had shown that the NSm polypeptide, which lies between Gn and Gc in the M polyprotein, was dispensable for virion production (28). Furthermore, we observed that Gn from cells transfected with a plasmid encoding HA-tagged M polyprotein migrated more slowly in SDS-PAGE than Gn from cells transfected with the HA-Gn^{313} plasmid (Fig. 1B), consistent with the two proteins having different masses.

BUNV Gn maturation occurs in a stepwise fashion, with Gn first being liberated from the rest of the M polyprotein via cleavage by signal peptidase between residues 331–332 (equivalent to OROV residues 335–336) to produce an immature Gn protein with two predicted TMDs, the second of TMD representing the NSm signal peptide (SP^{NSm}) and being subsequently removed by signal peptide peptidase (SPP) to yield mature Gn with a carboxy terminus at approximately residue 312 (29). Analysis of the OROV M polypeptide sequence using the SignalP 5.0 server (32) suggested that OROV Gn may also be liberated from the M polyprotein via cleavage by signal peptidase between residues G335 and E336 (Fig. 1A, second arrow). We therefore exploited an additional expression construct we had generated that included this predicted TMD, comprising the OROV M SS and HA-tag followed by M polypeptide residues 17–339 (Gn^{339}). While Gn^{339} was not secreted into the medium following expressed on its own in HEK293T cells, both Gn^{339} and Gc were abundant in the supernatant of cells co-transfected with constructs encoding both proteins (Fig. 1C). Co-expression of Gc with Gn^{339} is thus sufficient to promote release of both proteins from cells, presumably as VLPs or as exocytic vesicles. To test whether the two predicted TMDs plus cytosolic region of Gn^{339} were sufficient to promote Gc secretion, HEK293T cells were co-transfected with expression constructs encoding HA-tagged Gc and Gn residues 203–339 (GnCT). Neither Gc nor GnCT was secreted to the supernatant of these co-transfected cells, indicating that GnCT is not sufficient to promote secretion of Gc (Fig. 1C). To allow direct comparison

161 between Gn produced via recombinant expression and following OROV infection, an antibody was
162 raised against Gn residues 99–112 and recombinant constructs encoding Gc, Gn^{313}, Gn^{339} and the M
163 polyprotein with the OROV SS but no N-terminal epitope tag were cloned. Immunoblotting of HEK293T
164 cells transfected with M polyprotein, Gn^{313}+Gc, Gn^{339}+Gc, or infected with OROV (MOI = 1)
165 demonstrates that Gn from cells transfected with Gn^{339}, with M polyprotein or infected with OROV all
166 display equivalent electrophoretic mobility, whereas Gn^{313} migrates substantially faster (Fig. 1D).
167 Together, these results demonstrate that recombinant OROV glycoproteins are secreted when co-
168 expressed as individual proteins or as a polyprotein, but unlike BUNV the second TMD of OROV Gn is
169 not liberated by SPP following either recombinant expression or infection (Fig 1E).

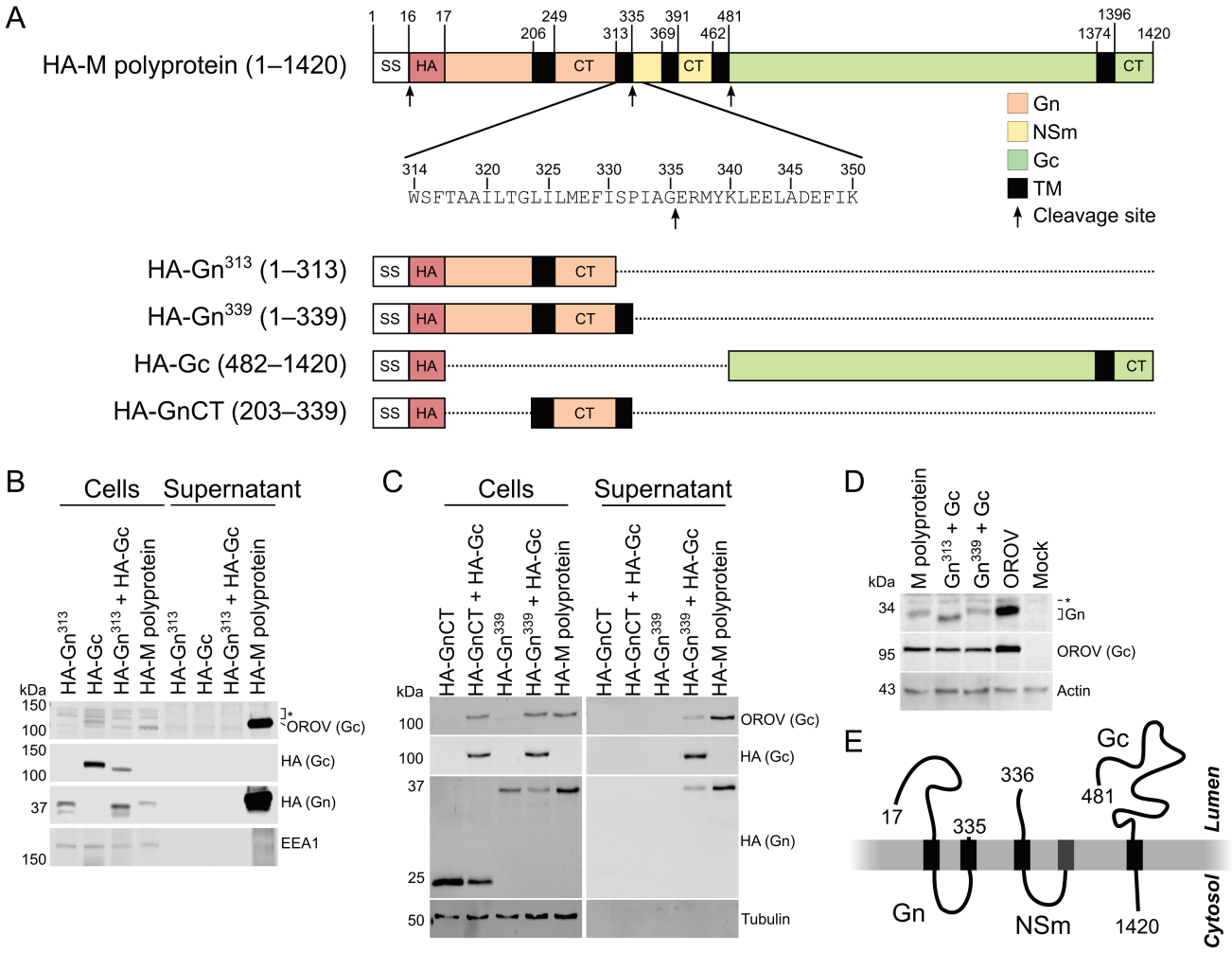

170 **Figure 1. Recombinant production and secretion of OROV glycoproteins.** (**A**) Schematic
171 representation of the recombinant constructs used to express the OROV M polyprotein, individual
172 glycoproteins or domains thereof. Expression constructs were preceded by the OROV M secretion
173 signal sequence (SS; unshaded) and an HA epitope tag (HA; red shading). Regions corresponding to
174 Gn, NSm and Gc are shaded in orange, yellow and green, respectively, with cytosolic tails denoted
175 (CT). Transmembrane regions (black) as predicted by TMHMM (31) and polyprotein cleavage sites
176 (arrows) are shown. (**B** and **C**) HEK293T cells were transfected with HA-tagged OROV M (poly)protein
177 constructs. After 48 h cell lysates and supernatants were harvested, subjected to SDS-PAGE and
178 immunoblotted using anti-HA and anti-OROV antibodies to detect secreted proteins, the latter
179 polyclonal antibody detecting Gc but not Gn, and with anti-EEA1 (**B**) or anti-tubulin (**C**) antibodies used
180 as loading controls. Data is representative of two (**B**) or three (**C**) independent experiments. Non-
181 specific bands are marked (*). (**D**) HEK293T cells were transfected with OROV M (poly)proteins lacking

182 an N-terminal epitope tag or infected with OROV (MOI = 1). After 24 h cells were harvested and
183 subjected to SDS-PAGE and immunoblotting using antibodies shown, anti-actin serving as a loading
184 control. Non-specific band is marked (*). Data is representative of four independent experiments. (**E**)
185 Schematic representation of OROV M polyprotein processing.

186 *The Gn^{339}:Gc complex is sufficient for Golgi localization*

187 During infection, the orthobunyavirus M polyprotein is translated at the ER before the Gn and Gc
188 proteins are transported to the Golgi apparatus, which is the main site of virus assembly (5). In order to
189 investigate the subcellular distribution of recombinant OROV glycoproteins (Fig. 1A), HeLa cells were
190 transfected with HA-tagged OROV glycoproteins and then stained for the HA signal and for the ER
191 chaperone calnexin 2 (CNX2) or the *cis*-Golgi marker GM130 (Fig. 2). When expressed alone, HA-
192 tagged Gn^{313}, Gc and Gn^{339} all co-localized with CNX2 at the ER and did not co-localise with GM130 at
193 the Golgi (Fig. 2A–C). Similarly, when HA-tagged Gn^{313} and Gc were co-expressed they were retained
194 at the ER and did not co-localise at the Golgi (Fig. 2D). However, when HA-tagged Gn^{339} and Gc were
195 co-expressed they showed extensive co-localisation with GM130 at the Golgi and less-extensive co-
196 localisation with CNX2 at the ER (Fig. 2E). Extensive GM130 co-localisation was also observed when
197 the HA-tagged OROV M polyprotein was expressed (Fig. 2F). Additionally, HA-stained puncta could
198 often be observed outside cells transfected with M polyprotein (Fig. 2F), suggesting that secreted
199 glycoproteins adhered to the coverslip during fixation and subsequent preparation of the microscope
200 slides. Taken together, these data indicate that co-expression of Gc with Gn spanning the first two
201 predicted TMDs (residues 1–339; Gn^{339}), either as separate polypeptides or as a polyprotein, is
202 necessary and sufficient for these proteins to be transported from the ER to the Golgi apparatus.

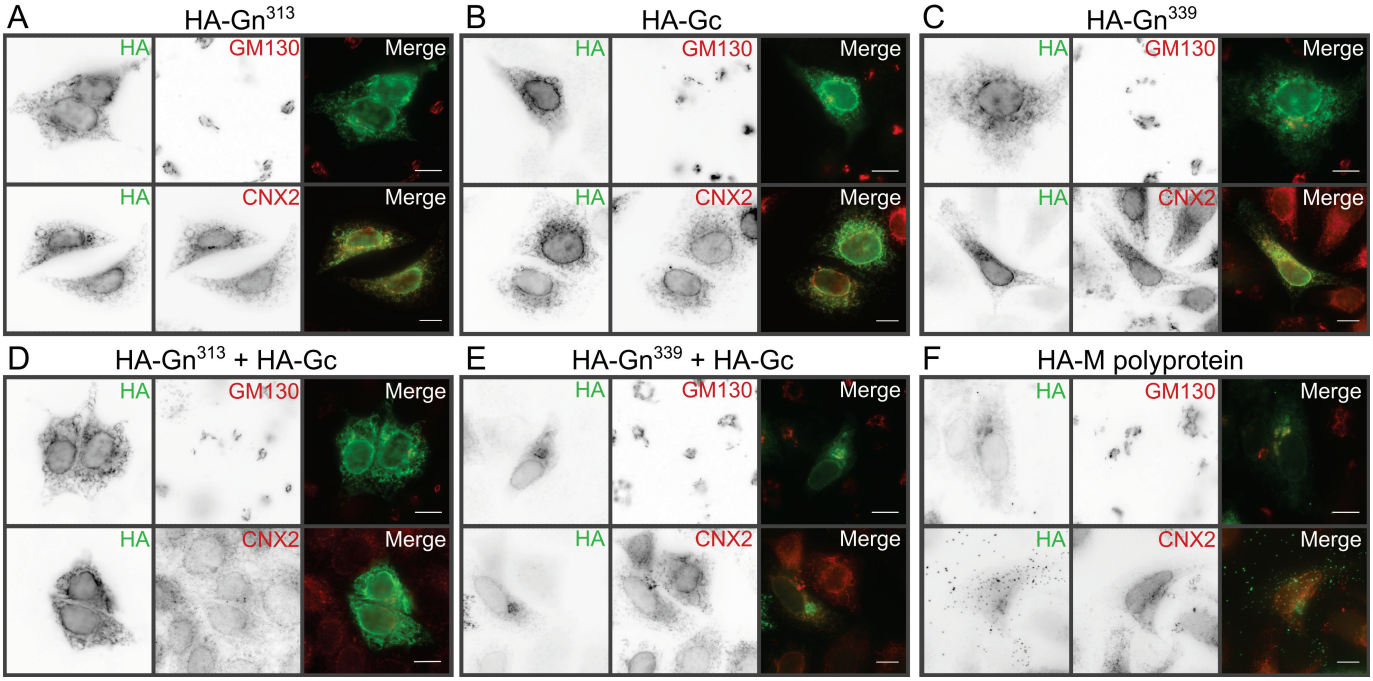

203 **Figure 2. Intracellular localization of OROV glycoproteins.** (**A** to **F**) HeLa cells were transfected with
204 plasmids expressing the HA-tagged OROV glycoproteins or the M polyprotein (as indicated). Cells were
205 fixed and co-stained with rabbit anti-HA (AF488) and either mouse anti-GM130 (AF568) or mouse anti-
206 CNX2 (AF568) antibodies to identify Golgi and ER compartments, respectively, before analysis using
207 wide-field fluorescence microscopy. Scale bars = 10 µm.

208 *Inhibition of the post-Golgi transport disrupts OROV glycoprotein secretion*

209 The OROV assembly pathway involves the recruitment of the host ESCRT machinery to Golgi
210 membranes for virus particle production (6). To further investigate the intracellular trafficking of the
211 OROV M polyprotein, two drugs were used to interfere with different steps of Golgi transport: Brefeldin
212 A was used to inhibit ER to Golgi transport, and monensin was used to block post-Golgi transport (33,
213 34). HEK293T cells were transfected with HA-tagged OROV M and the culture medium was collected
214 before and after drug treatment to monitor glycoprotein secretion. Secretion of OROV glycoproteins
215 was severely disrupted in cells treated with monensin or brefeldin A (Fig. 3A,B). Microscopic analysis
216 of drug-treated HeLa cells using the *cis*-Golgi marker GM130 (Fig. 3C) showed that brefeldin A caused
217 the anticipated dispersal of the *cis*-Golgi (35) and it prevented co-localisation of GM130 with the OROV
218 glycoproteins. Conversely, monensin treatment led to strong co-localisation of the glycoproteins with
219 enlarged and/or fragmented GM130-positive structures (Fig. 3C), osmotic swelling and fragmentation
220 of the Golgi being a consequence of monensin treatment (34). These results demonstrate that correct
221 Golgi function is required for OROV glycoprotein secretion.

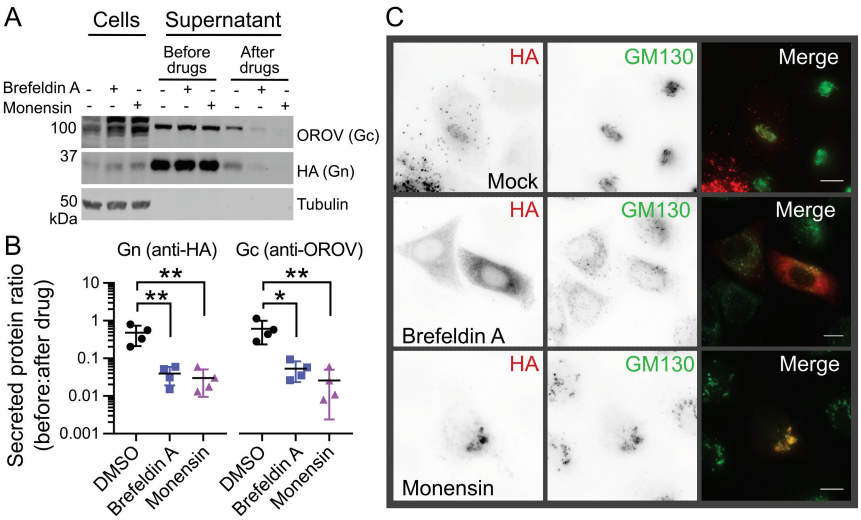

222

223 **Figure 3. Disruption of the Golgi apparatus prevents OROV glycoprotein secretion.** (**A**) HEK293T
224 cells were transfected with HA-tagged OROV M polyprotein and after 18 h the cell supernatant was
225 harvested and reserved. The culture medium was replenished and supplemented with 5 µg/mL brefeldin
226 A, 1 µM monensin or DMSO as a control. After 6 h, cells and supernatant were harvested. All samples
227 were then subjected to SDS-PAGE and immunoblotted using antibodies shown, anti-tubulin acting as
228 a loading control. (**B**) Ratio of Gn (anti-HA) and Gc (anti-OROV) protein present in supernatants
229 collected before or after drug treatment. Mean ± SD is shown for four independent experiments. *, $p \leq$
230 0.05; **, $p \leq 0.01$ (One-way ANOVA using Dunnett's test for multiple comparisons to DMSO control
231 cells). (**C**) HeLa cells transfected and drug treated as in (**A**) before fixation, co-staining with rabbit anti-
232 HA (AF568) plus mouse anti-GM130 (AF488) to identify Golgi membranes and analysis using wide-
233 field fluorescence microscopy. Scale bars = 10 µm.

234 *OROV glycoproteins secretion requires ESCRT machinery*

235 During OROV infection, multiple ESCRT components are recruited to Golgi membranes in order to
236 promote virus particle production (6). VPS4 is a cellular ATPase that stimulates the disassembly of

237 assembled ESCRT-III filaments at the necks of vesicles budding away from the cytoplasm, promoting
238 membrane scission (10). VPS4 is recruited to Golgi membranes during OROV infection and the
239 morphology of OROV viral factories is altered when infected cells express a dominant negative form of
240 this enzyme (VPS4E/Q) that inhibits ESCRT-III disassembly (6). In order to analyse whether secretion
241 of OROV glycoproteins is VPS4-dependent, HA-tagged OROV M polyprotein was transfected into
242 HEK293 cells stably expressing GFP-tagged wild-type human VPS4 or a dominant negative E228Q
243 mutant (VPS4E/Q) under the control of ecdysone response elements (36). Following transfection with
244 plasmids encoding HA-tagged OROV M polyprotein these VPS4-expressing cells, and the parental
245 control cells, were treated with either ponasterone A (Pon A) to induce VPS4 expression or with DMSO
246 as a vehicle control and the abundance of cell-associated and secreted OROV proteins was monitored
247 by immunoblotting (Fig. 4A). The secretion of Gn and Gc by parental cells and those expressing wild-
248 type GFP-VPS4 did not significantly differ when cells were treated with Pon A or DMSO (Fig. 4B). Gn
249 and Gc secretion was decreased when GFP-VPS4E/Q cells were treated with Pon A, although only the
250 decrease in Gn was statistically significant (Fig. 4B). To probe whether VPS4 activity was also required
251 for OROV virus particle release, the VPS4-expressing HEK293 cells were infected with OROV (MOI =
252 1) for 4 h before induction of VPS4 expression and analysis of cell-associated plus secreted OROV
253 protein abundance at 24 h post-infection (Fig. 4C). Both Gc and N protein secretion was significantly
254 decreased in GFP-VPS4E/Q cells treated with Pon A following infection with OROV, whereas Pon A
255 treatment of the parental or GFP-VPS4wt expressing cells did not alter OROV protein secretion (Fig.
256 4D).

257 OROV glycoproteins and GFP-tagged VPS4E/Q co-localised near GM130-positive *cis*-Golgi
258 membranes when the Pon A treated HEK293 stable cells were transfected with HA-tagged OROV M
259 polyprotein (Fig. 4E), similar to previous observations in OROV-infected HeLa cells (6), but unlike
260 previous studies GFP-tagged wild-type VPS4 did not co-localise with either OROV glycoproteins or the
261 Golgi marker GM130 (Fig. 4E). However, there was partial co-localisation between OROV glycoproteins
262 and wild-type VPS4 near Golgi (GM130- and TGN46-positive) membranes when HeLa cells were co-
263 transfected with YFP-tagged VPS4 and OROV M polyprotein (Fig. 4F). Taken together, these results
264 are consistent with VPS4 activity being required for OROV glycoprotein/virion secretion and with the
265 extent of fluorescently-tagged VPS4 localisation at the Golgi differing between HEK293 and HeLa cells.

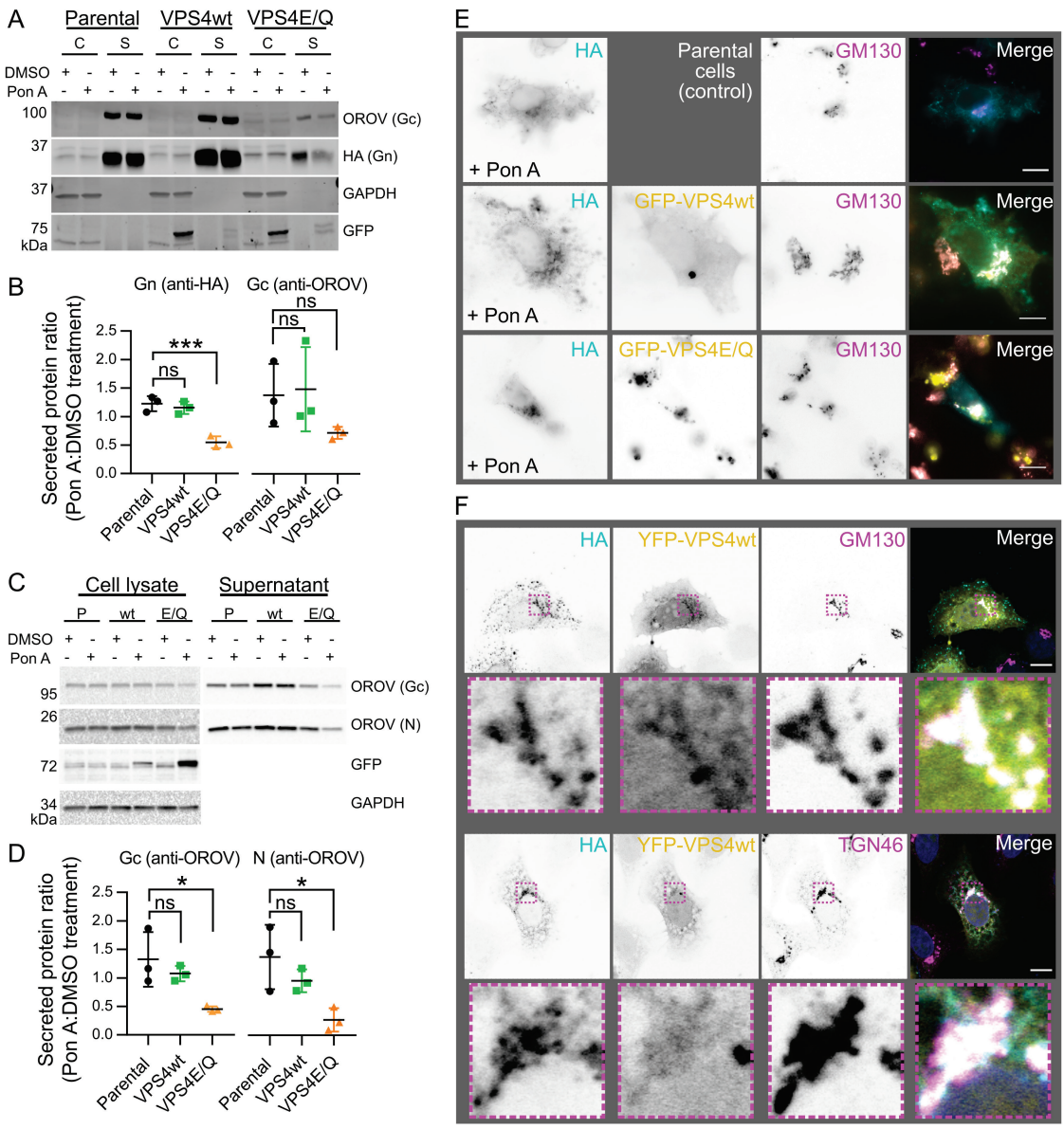

Figure 4. OROV protein secretion depends on VPS4 activity. (**A**) HEK293 cells stably expressing GFP-tagged wild-type VPS4 (VPS4wt) or a dominant negative mutant (VPS4E/Q) under the control of the ecdysone response element, or parental cells as a control, were transfected with HA-tagged M polyprotein and treated with either 1 µM ponasterone A (Pon A) or with DMSO as a control. After 48 h, cells (C) and supernatant (S) were harvested, subjected to SDS-PAGE and immunoblotted using antibodies shown. (**B**) Quantitation of the ratio of OROV Gn (anti-HA; left) or Gc (anti-OROV; right) that was secreted following treatment with Pon A versus DMSO. Mean ± SD from three independent experiments is shown. ***, $p \leq 0.001$ (One-way ANOVA using Dunnett's test for multiple comparisons to parental control cells). (**C**) HEK293 cells stably expressing VPS4wt (wt) or VPS4E/Q (E/Q) under the control of the ecdysone response element, or parental cells (P) as a control, were infected with OROV (MOI = 1) and after 4 h were treated with 1 µM Pon A or DMSO as a control. After 24 h cells and supernatant were harvested, subjected to SDS-PAGE and immunoblotted using antibodies shown, anti-OROV detecting both N and Gc proteins. (**D**) Quantitation of the ratio of OROV Gc (left) and N (right) secretion in cells treated with Pon A versus DMSO. Mean ± SD from three independent experiments is shown. *, $p \leq 0.05$ (One-way ANOVA using Dunnett's test for multiple comparisons to parental control cells). (**E**) HEK293 cells expressing GFP-tagged VPS4wt or VPS4E/Q, or parental cells, were transfected with HA-tagged OROV M polyprotein and treated with 1 µM Pon A for 18 h before being fixed and co-stained with rabbit anti-HA (AF568) and mouse anti-GM130 (AF647) antibodies and then analysed by wide-field fluorescence microscopy. Scale bars = 10 µm. (**F**) HeLa cells were co-transfected with plasmids expressing HA-tagged OROV M polyprotein and YFP-VPS4wt. After 24 h

286 cells were fixed and co-stained with rabbit anti-HA (AF568) and (top) mouse anti-GM130 (AF647) or
287 (bottom) sheep anti-TGN46 (AF647), and then analysed by confocal microscopy. Scale bars = 10 µm.

288 To further investigate the interaction between ESCRT-III components and OROV glycoproteins, HeLa
289 cells were transiently co-transfected with HA-tagged OROV M polyprotein and dominant-negative C-
290 terminally YFP tagged members of the charged multivesicular body protein (CHMP) family (37).
291 Although no co-localisation could be detected with the majority of CHMP proteins, partial co-localisation
292 could be observed between OROV glycoproteins and CHMP6-YFP (Fig. 5). A similar pattern of partial
293 co-localisation could be observed between OROV glycoproteins and endogenous CHMP6 (Fig. 6A),
294 the co-localisation of both endogenous and YFP-tagged CHMP6 with OROV glycoproteins being more
295 prominent when cells were treated with monensin to stall glycoprotein trafficking at the Golgi (Fig. 6A,B).

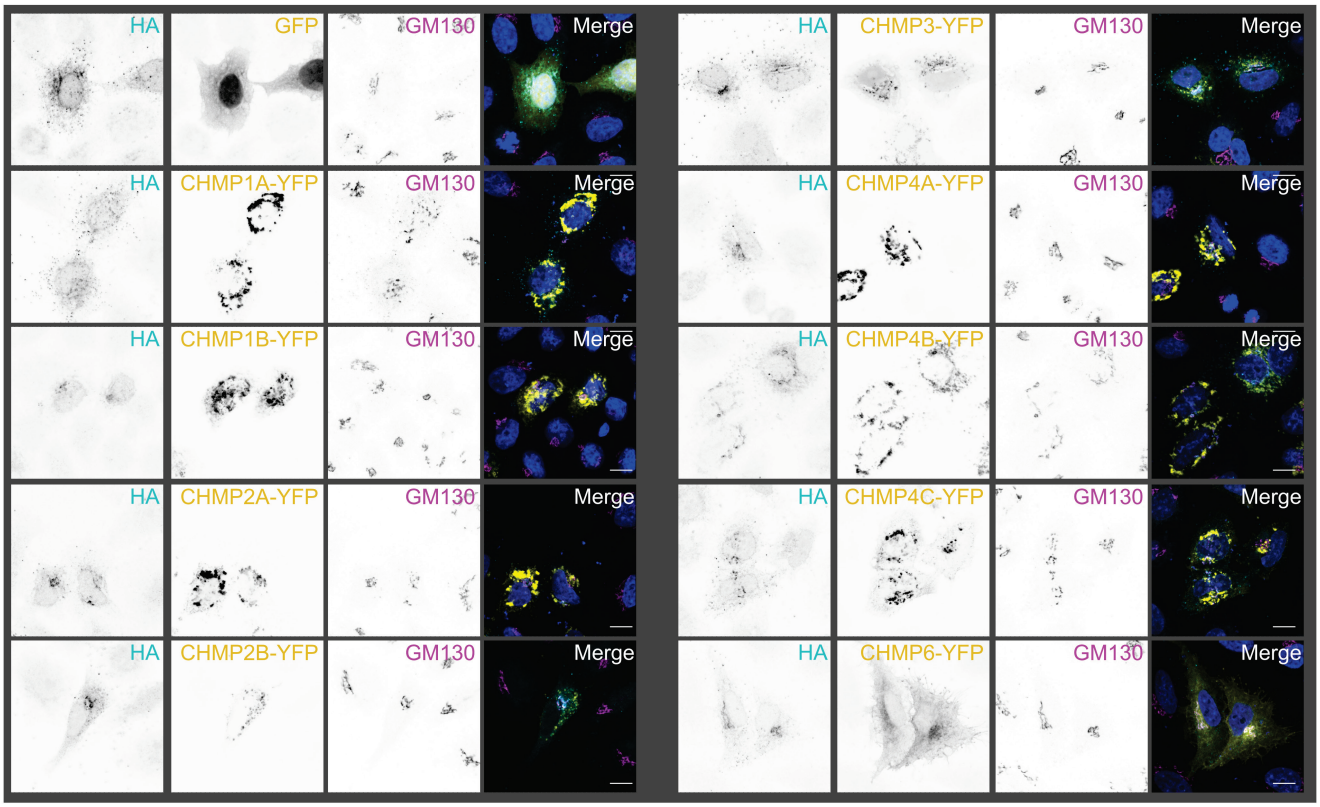

296 **Figure 5. OROV glycoproteins co-localise with CHMP6 but not with other ESCRT-III components.**
297 HeLa cells were co-transfected with plasmids expressing HA-tagged OROV M polyprotein and YFP-
298 tagged CHMP proteins (as indicated). After 24 h cells were fixed and co-stained with rabbit anti-HA
299 (AF568) and mouse anti-GM130 (AF647), and analysed by confocal microscopy. Scale bars = 10 µm.

300 CHMP6 nucleates the polymerisation of ESCRT-III filaments (9) and overexpression of CHMP6-YFP
301 confers a mild reduction in ESCRT-mediated secretion of HSV-1 and HIV-1 (38). OROV glycoprotein
302 secretion is significantly impaired when HEK293T cells are co-transfected with HA-tagged M polyprotein
303 and CHMP6-YFP versus GFP (Fig. 6C,D). Immunoprecipitation of co-transfected HEK293T cells
304 demonstrates that CHMP6 physically interacts with OROV glycoproteins: HA-tagged OROV
305 glycoproteins co-precipitate with CHMP6-YFP captured on GFP affinity resin (Fig. 6E) and CHMP6-
306 YFP co-precipitates with OROV glycoproteins captured using HA affinity resin (Fig. 6F). In both cases
307 co-precipitation is not observed with GFP or with CHMP5-YFP, confirming that the interaction is

308 specific. These data demonstrate that the ESCRT-III component CHMP6 interacts with OROV
309 glycoproteins, and that this interaction may promote glycoprotein secretion.

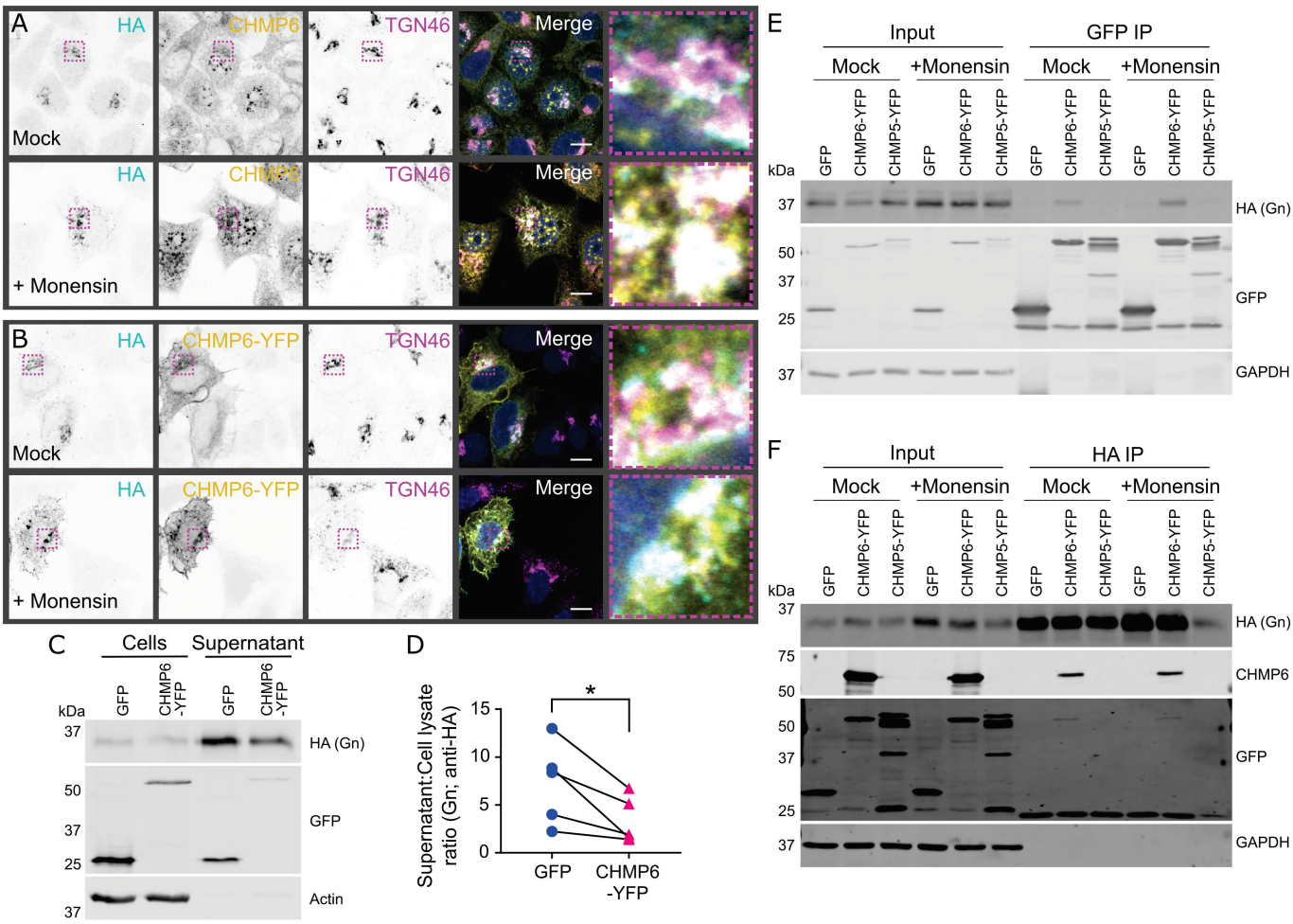

310 **Figure 6. OROV glycoproteins interact with CHMP6.** (**A**) HeLa cells were transfected with HA-tagged
311 OROV M polyprotein. After 18 h, cells were treated with 1 μM monensin or mock-treated for 6 h before
312 being fixed and co-stained with mouse anti-HA (AF568), rabbit anti-CHMP6 (AF488) and sheep anti-
313 TGN46 (AF647) before analysis by confocal microscopy. Scale bars = 10 μm. (**B**) HeLa cells were co-
314 transfected with HA-tagged OROV M polyprotein and YFP-tagged CHMP6. Cells were drug treated and
315 fixed as in (A) before staining with rabbit anti-HA (AF568) and sheep anti-TGN46 (AF647) before
316 analysis by confocal microscopy. Scale bars = 10 μm. (**C**) HEK293T cells were co-transfected with HA-
317 tagged M polyprotein and GFP or CHMP6-YFP. After 48 h cells and supernatant were harvested,
318 subjected to SDS-PAGE and immunoblotted using antibodies listed. (**D**) Ratio of Gn (anti-HA) signal in
319 the culture supernatant versus cell lysate. Data are from five independent experiments. *, $p \leq 0.05$
320 (paired ratio t test). (**E,F**) HEK293T cells were co-transfected with HA-M polyprotein and either GFP,
321 CHMP6-YFP or CHMP5-YFP. After 18 h, cells were treated with 1 μM monensin or mock-treated for
322 6 h. Cells were harvest and lysates subjected to affinity capture (IP) using either GFP (**E**) or HA (**F**)
323 affinity matrices before SDS-PAGE and immunoblotting using the antibodies shown. Representative
324 blots from two (**E**) or three (**F**) independent experiments are shown.

325 **Discussion**

326 We have characterized the maturation and secretion of OROV glycoproteins to study virus assembly
327 and budding. Surface glycoproteins are the principal viral components necessary for VLP production
328 across other members of the order *Bunyavirales* (19, 20). We demonstrate that OROV glycoproteins
329 are secreted when Gc is co-expressed with Gn but that the proteolytic processing of OROV Gn differs
330 from that of other orthobunyaviruses. Glycoprotein secretion is inhibited by drugs that interfere with
331 Golgi function. Secretion is also inhibited when the cellular ESCRT machinery is disrupted, and the
332 ESCRT-III component CHMP6 physically interacts with OROV glycoproteins.

333 Previous studies of BUNV have shown two cleavage sites between the boundaries of Gn and NSm in
334 the M polyprotein, either side of the second TMD (29). Specifically, Shi and colleagues (29) observed
335 that the second TMD of the BUNV M polyprotein (which they term SP^{NSm}) acts as a signal peptide for
336 NSm, being cleaved at its C terminus by cellular signal peptidases, and that this TMD is subsequently
337 liberated from the mature Gn protein by SPP. The migration of BUNV Gn in SDS-PAGE changed
338 linearly when Gn was truncated before the start of the second TMD, but the recombinant protein
339 migrated identically to mature Gn from BUNV infection or M polyprotein expression when stop codons
340 were introduced at or following the start of this second TMD. In contrast, we observe that the
341 electrophoretic mobility of Gn^{339}, which includes the second predicted TMD, matches that of Gn from
342 M polyprotein expression or OROV infection whereas the migration of untagged OROV Gn^{313} is faster,
343 consistent with Gn^{313} being a truncated form of Gn (Fig. 1D). Furthermore, we observe the efficient
344 secretion of OROV glycoproteins into the culture medium when Gn^{339} is co-expressed with Gc or when
345 OROV M is expressed as a polyprotein, but not when Gn^{313} is co-expressed with Gc. Taken together,
346 these data show that the OROV M polyprotein is processed to a mature Gn protein spanning two TMDs
347 (Gn^{335}), both in the context of recombinant polyprotein expression and during OROV infection. This
348 contrasts with previous observations for BUNV and suggests that the individual orthobunyaviruses have
349 differing requirements for cleavage of the second Gn TMD by SPP.

350 In addition to differences in proteolytic processing of the M polyprotein between BUNV and OROV, we
351 observed a difference in the requirement for co-expression of Gn and Gc in order for these proteins to
352 traffic from the ER to the Golgi. BUNV Gn is trafficked to the Golgi complex when expressed alone (8)
353 due to the Golgi retention signal located on its first TMD (39). In contrast, we observe that neither Gn
354 with either one or two predicted TMDs (Gn^{313} and Gn^{339}, respectively) nor Gc localise to the Golgi when
355 expressed in isolation. Co-expression of Gc with Gn^{339} (two predicted TMDs) resulted in strong co-
356 localisation of the glycoproteins with the *cis*-Golgi marker GM130, as did expression of the entire M
357 polyprotein. The difference in requirement for Gn and Gc co-expression in order to mature beyond the
358 ER into the Golgi may highlight structural differences between the orthobunyavirus glycoproteins, with
359 the BUNV Gn extracellular domain being capable of folding independently whereas the OROV Gn
360 extracellular region requires Gc for folding and/or stabilisation.

361 Since bunyaviruses do not possess matrix proteins, the cytosolic tails of Gn and Gc are believed to be
362 important for virus assembly and budding. The Gn cytosolic domain of Uukuniemi phlebovirus interacts
363 with virus ribonucleoprotein, which is crucial for genome packaging (40). Furthermore, the Gn and Gc
364 cytosolic tails of BUNV are required for Golgi complex targeting, virus assembly and infectivity (41),
365 with the first TMD of BUNV Gn being required for correct Golgi targeting of Gc (39). We therefore
366 investigated whether the Gn cytosolic tail (residues 203–339, GnCT) could serve as a chaperone for
367 Gc. Gc is not secreted into the medium when co-expressed with GnCT, whereas co-expression of Gc
368 with Gn^{339} did promote glycoprotein secretion (Fig. 1C). This data confirms that the Gn^{339} extracellular
369 domain is required for secretion of Gc, consistent with previous studies of BUNV showing that mutations
370 in the glycosylation sites of Gn prevented correct folding of both Gn and Gc (42).

371 Previous studies of BUNV showed that budding and initial maturation steps occur in the Golgi stacks,
372 but that full virus maturation does not proceed without a functional *trans*-Golgi (7). Fragmentation of the
373 Golgi is observed when Vero cells are infected with BUNV, although these fragmented Golgi are still
374 competent to sustain infectious virion production (7). Similarly, OROV infection leads to *trans*-Golgi
375 network fragmentation as detected by dispersion of the TGN46 marker (6). We do not observe
376 fragmentation of the Golgi in cells expressing the M polyprotein (Figs 2F and 6A), suggesting that
377 additional OROV proteins are required to promote Golgi fragmentation. Two drugs that interfere with
378 the Golgi complex via different mechanisms were used to investigate the intracellular trafficking of
379 OROV glycoproteins. The drug monensin strongly disrupts *trans*-Golgi network function by altering the
380 pH (34), allowing us to probe post-Golgi transport of glycoproteins (Fig. 3). We observed an
381 accumulation of intracellular glycoproteins at GM130-positive compartments in monensin-treated cells
382 with a concomitant drop in glycoprotein secretion into the extracellular medium, confirming that a
383 functional *trans*-Golgi network is required for OROV glycoprotein maturation and secretion. Brefeldin A
384 prevents protein traffic from the ER to the Golgi but allows retrograde trafficking to proceed, causing re-
385 adsorption of the Golgi into the ER (35). As expected, we observed a loss of the distinct Golgi-like
386 staining patterns for both the OROV glycoproteins and the *cis*-Golgi marker GM130, plus a loss of
387 glycoprotein secretion, following brefeldin A treatment (Fig. 3C). Interestingly, we do not observe
388 accumulation of intracellular glycoproteins, consistent with a loss in protein translation caused by the
389 ER stress induced by brefeldin A treatment (43). Taken together, our data show disruption of Golgi
390 function inhibits OROV glycoprotein maturation and secretion, as has been observed previously for
391 cells infected with BUNV (44).

392 The production of OROV infectious particles requires the cellular ESCRT machinery (6). To probe
393 whether OROV glycoprotein secretion also requires ESCRT activity, and thus faithfully recapitulates
394 infectious virus particle production, we investigated the association of ESCRT components with OROV
395 glycoproteins and role of the cellular ESCRT machinery in viral glycoprotein secretion. The ESCRT-III–
396 disassembling ATPase VPS4 co-localises with OROV replication sites, expression of the ATPase-
397 defective VPS4E/Q mutant leading to changes in replication compartment morphology (6). Secretion of
398 OROV glycoproteins is decreased when cells express VPS4E/Q, whereas secretion from parental cells
399 or those expressing wild-type VPS4 is unchanged (Fig. 4A,B). Furthermore, a similar decrease in

400 secretion of OROV Gc and N (presumably as virions) is observed during infection in VPS4E/Q-
401 expressing cells versus parental and wild-type VPS4 expressing cells (Fig. 4C,D). This strongly
402 suggests that VPS4 activity promotes OROV viral glycoprotein and virion secretion. Interestingly, while
403 GFP-VPS4E/Q co-localized with OROV glycoproteins at Golgi membranes in HEK293 cells (Fig. 4E) in
404 a similar manner to OROV infectious particles (6), GFP-VPS4wt did not. However, overexpression in
405 HeLa cells yields co-localisation of YFP-VPS4wt with OROV glycoproteins and Golgi membranes (Fig.
406 4F), as observed previously for OROV infectious particles (6), consistent with the steady-state
407 abundance of co-localised OROV glycoproteins and VPS4 differing between different cell types.

408 To further understand how cellular ESCRT components may promote OROV glycoprotein secretion,
409 we investigated the co-localisation of OROV glycoproteins with overexpressed, dominant-negative
410 YFP-tagged cellular ESCRT-III components (Fig. 5). Partial co-localisation was observed with both
411 YFP-tagged and endogenous CHMP6 (Figs 5 and 6A), a myristoylated protein that nucleates ESCRT-
412 III polymerisation (9), and co-immunoprecipitation experiments demonstrate a physical interaction
413 between OROV glycoproteins and CHMP6-YFP (Fig. 6E,F). Most enveloped viruses that recruit the
414 cellular ESCRT membrane-remodelling machinery for budding do so using peptide motifs known as
415 viral 'late domains' (13, 14), but the OROV structural proteins lack identifiable late domain sequences.
416 The Bro1-domain containing protein ALIX and ESCRT-I component TSG101, which act in parallel to
417 stimulate ESCRT-III polymerisation (9), both contribute to OROV viral factory morphogenesis and virus
418 production (6). Demonstration that OROV glycoproteins physically interact with CHMP6 raises the
419 interesting hypothesis that OROV might also recruit CHMP6 directly to further enhance ESCRT-III
420 polymer formation on Golgi membranes. Hijacking of cellular ESCRT activity via by direct stimulation
421 of ESCRT-III polymerisation, rather than via late domain mediated recruitment of ESCRT adaptors, has
422 been hypothesised for herpesviruses (45, 46) but remains to be shown definitively. Overexpression of
423 CHMP6-YFP significantly decreases the secretion of OROV glycoproteins (Fig. 6C,D). While this is
424 consistent with the tagged CHMP6 protein having a dominant negative effect upon ESCRT-mediated
425 OROV glycoprotein secretion, it does not differentiate between ESCRT-III activity being stimulated via
426 ESCRT-I/ESCRT-II mediated recruitment or by direct CHMP6 binding to OROV glycoproteins. Further
427 experiments are required to dissect the molecular mechanisms by which ESCRT-III activity is stimulated
428 to promote OROV glycoprotein and virion secretion.

429 In summary, we have demonstrated that OROV Gn contains two predicted TMDs that are essential for
430 OROV glycoprotein trafficking to the Golgi complex. Pharmacological disruption of Golgi function
431 inhibits OROV glycoprotein secretion, as do perturbations of ESCRT complex function. Furthermore,
432 we observe co-localisation and interaction of CHMP6 of the ESCRT-III components with the OROV
433 glycoproteins, suggesting that OROV may directly stimulate ESCRT-III polymerisation to support virus
434 budding. *In vitro* expression of OROV glycoproteins represents a convenient experimental system for
435 analysing the cellular determinants of OROV assembly and budding, avoiding requirements for high-
436 containment biosecurity. The similarity in glycoprotein processing and requirement for VPS4 activity
437 suggests that OROV Gn and Gc co-expression outside the context of infection leads to glycoprotein

438 self-assembly and secretion from the cell as VLPs, although formal verification of this awaits future
439 electron microscopy analysis.

440 **Materials and Methods**

441 *Cell Culture*

442 Mycoplasma-free HeLa and HEK293T cells were maintained in Dulbeco's modified Eagle's medium
443 (DMEM; Gibco) supplemented with 10% heat-inactivated foetal calf serum (FCS) and 2 mM glutamine
444 at 37°C in a humidified 5% CO_2 atmosphere. HEK293 cells stably expressing the ecdysone receptor
445 (EcR-293; Invitrogen), and derived cell lines stably expressing GFP-tagged wild-type or dominant
446 negative (E228Q) human VPS4 under the control of ecdysone response elements, were maintained in
447 the medium listed above supplemented with 400 µg/ml Zeocin and 800 µg/ml G418 (36).

448 *Plasmids and Constructs*

449 All fragments of the M polyprotein from OROV strain BeAn19991 (GenBank ID KP052851.1) used in
450 this study were synthesised (GeneArt) following codon-optimization for expression in human cells.
451 Constructs encoding Gn^{313} (M polyprotein residues 1–313) and Gc (residues 482–1420) were
452 synthesised with an HA epitope tag and BamHI restriction sequence immediately following the Gn
453 secretion signal sequence (SS), and were cloned into pcDNA3.1(+) using the restriction enzymes NheI
454 and XhoI. To generate the HA-tagged OROV M polyprotein construct, an extended NSm fragment (M
455 polyprotein residues 299–496) was synthesised to overlap with the N and C termini of Gc and Gn^{313},
456 respectively. The sequences for Gc, NSm and the entire pcDNA3.1 vector encoding Gn with an N-
457 terminal SS plus HA tag were amplified by PCR using KOD Hot Start DNA polymerase (Novagen),
458 mixed and then concatenated using the NEBuilder HiFi assembly kit according to the manufacturer's
459 instructions to yield pSnH-OROV-M. HA-tagged Gn^{339} was generated by site directed mutagenesis of
460 pSnH-OROV-M to insert a stop codon after residue 339 using the mutagenic primers listed in Table 1.
461 HA-tagged GnCT was amplified from pSnH-OROV-M using the primers shown in Table 1, digested with
462 the restriction endonucleases BamHI and Xhoi, and ligated into BamHI/XhoI digested pSnH-OROV-M
463 to yield the Gn SS and an HA epitope tag followed by M polyprotein residues 203–339. All expression
464 constructs were verified by Sanger sequencing. CHMP-YFP plasmids were as described previously
465 (38).

466 *Table 1. Oligonucleotide primers used in this study. Restriction sites are in **bold**.*

Name	Sequence (5′ to 3′)	Details
Gn C-terminal forward	CAAGAGCCTGAGCAAGGCCAG	Amplify NSm to generate HA-M polyprotein construct
Gc N-terminal reverse	CTTGGTAGGTGATCTTGATGTCCTTGC	Amplify NSm to generate HA-M polyprotein construct
pcDNA 3′ forward	CGTTTAAACCCGCTGATCAGC	Amplify Gn^{313} and pcDNA vector to generate HA-M polyprotein construct

Gn^{313} C-terminal reverse	GCTCTTGCTCTTGCACATCTGTC	Amplify Gn^{313} and pcDNA vector to generate HA-M polyprotein construct
Gc N-terminal forward	GATGAGGACTGCCTGAGCAAGGAC	Amplify Gc to generate HA-M polyprotein construct
BGH reverse	TAGAAGGCACAGTCGAGG	Amplify Gc to generate HA-M polyprotein construct
Gn^{339} forward	CGAGCGGATGTACTAGCTGGAAGAACTG	Generate Gn^{339} by replacing reside 340 of HA-M polyprotein with a stop codon
Gn^{339} reverse	CAGTTCTTCCAGCTAGTACATCCGCTCG	Generate Gn^{339} by replacing reside 340 of HA-M polyprotein with a stop codon
GnCT forward	GAA**GGATCC**GAGGCTATGTGCGTGAACATC	Clone HA-tagged GnCT
GnCT reverse	GGAA**CTCGAG**TCAGTACATCCGCTCGCCGGCAATG	Clone HA-tagged GnCT

Antibodies

For immunoblot analyses the following primary antibodies (identifier, dilution) were used: anti-GFP (Sigma G2544, 1:5000), anti-OROV (Gc detection; ATCC VR-1228AF, 1:1000), anti-OROV antiserum (Gc and N detection; kindly donated by Luis Tadeu Moraes Figueiredo, University of São Paulo, 1:500), anti-CHMP6 (kindly donated by Wesley Sundquist, University of Utah, 1:1000), anti-HA (Cell Signaling Technology C29F4, 1:20,000), anti-actin (Sigma A3853, 1:1000), anti-tubulin hybridoma supernatant (clone YL1/2) (47), anti-GAPDH (GeneTex GTX28245, 1:10000) and anti-EEA1 (Abcam Ab2900, 1:1000). The secondary antibodies were LI-COR IRDye 680T conjugated donkey anti-rabbit (926-68023) or goat anti-mouse (926- 68020), or LI-COR IRDye 800CW conjugated donkey anti-rabbit (926-32213) or goat anti-mouse (926-32210). Polyclonal serum against Gn was raised commercially (GenScript) by immunisation of rabbits with a synthetic peptide (Gn residues 99–112, sequence VLSVDDNGHIIPKMC) coupled to keyhole limpit hemocyanin, followed by affinity purification. This antibody was validated by immunoblotting lysates of HEK293T cells transfected with pSnH-OROV-M and was used at 1:1000 dilution. For immunocytochemistry the following primary antibodies (identifier, dilution) were used: anti-HA (Cell Signaling Technology C29F4, 1:1000), anti-GM130 (BD Biosciences 610822, 1:1000), anti-TGN46 (BioRad AHP500G, 1:250), anti-CHMP6 (kindly donated by Wesley Sundquist, University of Utah, 1:200), and anti-Calnexin2 (BD Biosciences 610523, 1:100). Secondary antibodies were Alexa Fluor conjugated goat anti-mouse (A-21236, A-11001 and A-11031, ThermoFisher), donkey anti-rabbit (A-10042, ThermoFisher), goat anti-rabbit (A-11008, ThermoFisher), donkey anti-mouse (A32766, ThermoFisher), and donkey anti-sheep (A21448, ThermoFisher).

OROV glycoprotein secretion and immunoblotting

HEK293T cells were seeded at 2.5×10^5 cells per well in six well dishes. Cells were transfected by mixing 2 µg of DNA (split evenly by mass between the plasmids indicated) and 1.5 µg of branched polyethylenimine (PEI; average MW ~25,000, Merck) in Opti-MEM (ThermoFisher), incubating at room temperature for 20 min and then applying to cells. Cell culture medium was harvested after 48 h and

493 cleared of cellular debris by centrifugation at 800×g for 10 min at 4°C. Glycoproteins in the supernatants
494 were pelleted by centrifugation at 100,000×g at 4°C for 90 min using a TLA-55 rotor (Beckman). The
495 resultant pellets, containing glycoproteins, were resuspended and boiled in sodium dodecyl sulfate-
496 polyacrylamide gel electrophoresis (SDS-PAGE) sample buffer. Cell samples were harvested by
497 centrifugation and resuspended in lysis buffer (10 mM Tris pH 7.5, 150 mM NaCl, 0.5% IGEPAL CA-
498 630 [a.k.a. NP-40], 0.5 mM EDTA) supplemented with EDTA-free protease inhibitor cocktail (Roche)
499 and incubated on ice for 30 min. Lysates were clarified by centrifugation at 20,000×g for 10 min at 4°C.
500 The protein concentration in each lysate sample was normalized following quantification using the BCA
501 assay (ThermoFisher) and samples were boiled in SDS-PAGE sample buffer. Samples were separated
502 by SDS-PAGE using 10% or 15% (w/v) polyacrylamide gels and transferred to Protran nitrocellulose
503 membranes (Perkin Elmer) using the Mini-Trans blot systems (BioRad) following the manufacturer's
504 protocol. After blocking in Intercept blocking buffer (LI-COR) for anti-Gn or PBS with 5% (w/v) non-fat
505 milk powder for all other antibodies, membranes were incubated with primary antibody at room
506 temperature for 1 h or overnight at 4°C, washed, and then incubated with the secondary antibody for
507 1 h at room temperature. Dried blots were visualized on an Odyssey CLx infrared scanner (LI-COR).
508 Statistical tests were performed using Prism version 7 (GraphPad).

509 For comparison of OROV glycoproteins from infection versus transfection, HEK293T cells were seeded
510 at $5x10^6$ cells per 9 cm dish and allowed to rest for 24 h. Cells were transfected by mixing 20 µg of DNA
511 (split evenly by mass between the plasmids indicated) and lipofectamine 2000 reagent according
512 manufacture's protocol. Alternatively, cells were infected with OROV (MOI = 1) in DMEM with 2% FCS
513 for 1 h at 4°C on a rocker. Media was then refreshed with DMEM containing 2% FCS (infection) or 10%
514 FCS (transfection). 24 h after transfection or infection, cell monolayers were rinsed with ice-cold PBS
515 and then lysed on the dish with 1 mL of lysis buffer (0.1% [v/v] IGEPAL CA-630 in PBS with protease
516 inhibitor cocktail [Sigma-Aldrich]) for 20 minutes on ice. Lysates were clarified by centrifugation
517 16000×g for 15 min at 4°C. The protein concentration in each lysate sample was quantified with Quick
518 Start Bradford 1× Dye (BioRad) to equalise protein concentrations across the samples before SDS-
519 PAGE and immunoblotting.

520 For glycoprotein isolation following drug treatment, HEK293T cells were transfected with a plasmid
521 expressing HA-tagged M polyprotein as described above. After 18 h, the culture medium was collected
522 and glycoproteins were isolated by ultracentrifugation as described above ("Before drugs"). The
523 medium was replaced with FreeStyle 293 medium (ThermoFisher) supplemented with 5 µg/mL brefeldin
524 A (Enzo Life Science BML-G405) or 1 µM monensin (Merck M5273) and cells were incubated for a
525 further 6 h before the supernatant and cell lysates were harvested and processed as described above
526 ("After drugs").

527 For glycoprotein isolation from ecdysone-responsive stable cell lines, cells were seeded differently.
528 Parental and GFP-VPS4wt EcR-293 cells were seeded at $5×10^6$ cells per 9 cm dish, whereas GFP-
529 VPS4E/Q EcR293 cells (which grow more slowly) were seeded at $8×10^6$ cells per 9 cm dish. Cells were
530 transfected with 7.7 µg of a plasmid expressing HA-tagged M polyprotein using TransIT-LT1 (Mirus)

531 and after 6 h the cells were treated with either DMSO or 1 μM ponasterone A (Pon A). After 18 h of
532 drug treatment, the medium was refreshed using FreeStyle 293 medium (ThermoFisher). Cell lysates
533 and supernatants were harvested at 48 h post-transfection and processed as described above.

534 For OROV infection of ecdysone-responsive stable cells lines, EcR-293 cells were seeded as described
535 above and infected with OROV (MOI = 1) in DMEM with 2% FCS for 1 h at 4°C on a rocker. Media was
536 then refreshed (DMEM with 2% FCS). After 4 h cells were treated with 1 μM Pon A (or DMSO as a
537 control) and after 24 h cells and supernatant were harvested as described previously (6).

538 *Co-immunoprecipitation of transfected cells*

539 HEK 293T cells were seeded at 5×10^6 cells per 9 cm dish. Cells were transfected with 7.7 μg of a
540 plasmid (split evenly by mass between the plasmids indicated) using TransIT-LT1 (Mirus) and after 18
541 h the cells were mock-treated (refreshed media) or treated with 1 μM monensin for 6 h. Cells were
542 pelleted (220 g, 5 min, 4°C), washed three times with cold PBS, and cell pellets were processed for
543 immunoprecipitation.

544 For GFP capture, cells were lysed at 4°C in 1 mL lysis buffer (10 mM Tris pH 7.5, 150 mM NaCl, 0.5
545 mM EDTA, 0.5% IGEPAL CA-630, EDTA-free protease inhibitor cocktail [Roche]) for 30 min before
546 clarification (20,000×g, 10 min, 4°C). For HA capture, cells were lysed at 4°C in 1 mL lysis buffer (10
547 mM Tris pH 7.5, 150 mM NaCl, 0.1% IGEPAL CA-630, EDTA-free protease inhibitor cocktail [Roche]).
548 Protein concentration in the lysates was quantified by BCA assay (ThermoFisher) to equalise protein
549 concentrations across the samples before immunoprecipitation with GFP-Trap resin (gta-20,
550 ChromoTek) or anti-HA affinity matrix (11815016001, Roche) following the manufacturers' protocols.
551 Cell lysate was immunoprecipitated for 2 h with GFP-TRAP or overnight with anti-HA affinity matrix, at
552 4°C under agitation. Input samples were collected prior to immunoprecipitation and represent 2% of the
553 total cell extract. Samples were eluted by incubation at 95°C for 5 min in 45 μL 2× SDS-PAGE loading
554 buffer. Input and bound samples were separated by SDS-PAGE and analysed by immunoblot.

555 *Immunocytochemistry*

556 HeLa cells were seeded on glass coverslips at a density of 5×10^4 cells per well in 24 well dishes. Cells
557 were transfected with 250 ng of DNA (split evenly by mass between the plasmids indicated) using
558 TransIT-LT1 (Mirus). Cells were either incubated for 24 h (untreated), or for 18 h whereupon the culture
559 medium was replenished with medium 1 μM monensin, 5 ug/mL brefeldin A or DMSO as a control
560 before incubation for a further 6 h. Cells were transferred onto ice and were washed with ice-cold PBS
561 and fixed with cold 250 mM HEPES pH 7.5, 4% (v/v) electron microscopy-grade formaldehyde (PFA,
562 Polysciences) for 10 min on ice before and then incubated with 20 mM HEPES pH 7.5, 4% (v/v) PFA
563 at room temperature for a further 20 min. After washing with PBS, cells were permeabilized by
564 incubation with 0.1% saponin in PBS for 30 min before being incubated with blocking buffer (5% [v/v]
565 FBS, 0.1% saponin in PBS) for 30 min. Primary antibodies were diluted in blocking buffer and incubated

566 with coverslips for 2 h. Coverslips were washed five times with blocking buffer before incubation for 1
567 h with the relevant secondary antibodies diluted in blocking buffer. Coverslips were washed five times
568 with blocking buffer, three times with 0.1% saponin in PBS, three times with PBS, and finally with
569 ultrapure water. Coverslips were mounted using Mowiol 4-88 (Merck) containing 200 nM 4′,6-diamidino-
570 2-phenylindole (DAPI) and allowed to set overnight. Cells were analysed on a Zeiss confocal laser
571 scanning microscope (LSM)780 (Zeiss) or on an Olympus IX81 wide-field fluorescence microscope.
572 Images were processed using Fiji (48, 49).

573 Ecdysone-responsive stable cell lines were seeded on poly-D-lysine treated glass coverslips at a
574 density of 2×10^4 cells per well in 24 well dishes. Cells were transfected with 250 ng of plasmid
575 expressing HA-tagged M polyprotein using TransIT-LT1 (Mirus) and after 6 h cells were treated with
576 1 μM Pon A or DMSO as a control. After 18 h of drug treatment, cells were processed as described
577 above.

578 **Acknowledgements**

579 The authors thank Susanna Colaco for superb technical assistance. This work was supported by
580 doctoral studentship and travelling fellowship from the Fundação de Amparo à Pesquisa do Estado de
581 São Paulo (FAPESP; 2016/18356-4 and 2019/02945-9) to NSB, by a FAPESP Pump Priming award
582 (2019/02418-9) to LLPdS, by a Biotechnology and Biological Sciences Research Council
583 (BBSRC)/FAPESP pump priming award (BB/S018670/1) to CMC, LLPdS and SCG, and by a Sir Henry
584 Dale Fellowship co-funded by the Royal Society and the Wellcome Trust (098406/Z/12/B) to SCG. The
585 funders had no role in study design, data collection and analysis, decision to publish, or preparation of
586 the manuscript. For the purpose of open access, the authors have applied a Creative Commons
587 Attribution (CC BY) licence to any Author Accepted Manuscript version arising from this submission.

588 **Conflict of Interest**

589 The authors declare they have no conflict of interest.

590 **References**

591 1. Sakkas H, Bozidis P, Franks A, Papadopoulou C. 2018. Oropouche Fever: A Review. Viruses
592 10:E175.
593 2. Romero-Alvarez D, Escobar LE. 2018. Oropouche fever, an emergent disease from the Americas.
594 Microbes Infect 20:135–146.
595 3. Gutierrez B, Wise EL, Pullan ST, Logue CH, Bowden TA, Escalera-Zamudio M, Trueba G, Nunes
596 MRT, Faria NR, Pybus OG. 2020. Evolutionary Dynamics of Oropouche Virus in South America.
597 J Virol 94:e01127-19.
598 4. Hughes HR, Adkins S, Alkhovskiy S, Beer M, Blair C, Calisher CH, Drebot M, Lambert AJ, de
599 Souza WM, Marklewitz M, Nunes MRT, Shí X, Ictv Report Consortium. 2020. ICTV Virus
600 Taxonomy Profile: Peribunyaviridae. J Gen Virol 101:1–2.
601 5. Elliott RM. 2014. Orthobunyaviruses: recent genetic and structural insights. Nat Rev Microbiol
602 12:673–685.
603 6. Barbosa NS, Mendonça LR, Dias MVS, Pontelli MC, da Silva EZM, Criado MF, da Silva-Januário
604 ME, Schindler M, Jamur MC, Oliver C, Arruda E, daSilva LLP. 2018. ESCRT machinery
605 components are required for Orthobunyavirus particle production in Golgi compartments. PLoS
606 Pathog 14:e1007047.
607 7. Salanueva IJ, Novoa RR, Cabezas P, López-Iglesias C, Carrascosa JL, Elliott RM, Risco C. 2003.
608 Polymorphism and structural maturation of bunyamwera virus in Golgi and post-Golgi
609 compartments. J Virol 77:1368–1381.
610 8. Lappin DF, Nakitare GW, Palfreyman JW, Elliott RM. 1994. Localization of Bunyamwera
611 bunyavirus G1 glycoprotein to the Golgi requires association with G2 but not with NSm. J Gen
612 Virol 75:3441–3451.
613 9. Christ L, Raiborg C, Wenzel EM, Campsteijn C, Stenmark H. 2017. Cellular Functions and
614 Molecular Mechanisms of the ESCRT Membrane-Scission Machinery. Trends Biochem Sci
615 42:42–56.
616 10. Maity S, Caillat C, Miguet N, Sulbaran G, Effantin G, Schoehn G, Roos WH, Weissenhorn W.
617 2019. VPS4 triggers constriction and cleavage of ESCRT-III helical filaments. Sci Adv
618 5:eaau7198.
619 11. Schöneberg J, Pavlin MR, Yan S, Righini M, Lee I-H, Carlson L-A, Bahrami AH, Goldman DH,
620 Ren X, Hummer G, Bustamante C, Hurley JH. 2018. ATP-dependent force generation and
621 membrane scission by ESCRT-III and Vps4. Science 362:1423–1428.
622 12. Effantin G, Dordor A, Sandrin V, Martinelli N, Sundquist WI, Schoehn G, Weissenhorn W. 2013.
623 ESCRT-III CHMP2A and CHMP3 form variable helical polymers in vitro and act synergistically
624 during HIV-1 budding. Cell Microbiol 15:213–226.
625 13. Freed EO. 2002. Viral late domains. J Virol 76:4679–4687.
626 14. Votteler J, Sundquist WI. 2013. Virus budding and the ESCRT pathway. Cell Host Microbe
627 14:232–241.
628 15. Tabata K, Arimoto M, Arakawa M, Nara A, Saito K, Omori H, Arai A, Ishikawa T, Konishi E, Suzuki
629 R, Matsuura Y, Morita E. 2016. Unique Requirement for ESCRT Factors in Flavivirus Particle
630 Formation on the Endoplasmic Reticulum. Cell Rep 16:2339–2347.
631 16. Vietri M, Radulovic M, Stenmark H. 2020. The many functions of ESCRTs. Nat Rev Mol Cell Biol
632 21:25–42.
633 17. Watanabe S, Watanabe T, Noda T, Takada A, Feldmann H, Jasenosky LD, Kawaoka Y. 2004.
634 Production of novel ebola virus-like particles from cDNAs: an alternative to ebola virus generation
635 by reverse genetics. J Virol 78:999–1005.
636 18. Strecker T, Eichler R, Meulen J ter, Weissenhorn W, Dieter Klenk H, Garten W, Lenz O. 2003.
637 Lassa virus Z protein is a matrix protein and sufficient for the release of virus-like particles. J Virol
638 77:10700–10705.
639 19. Acuña R, Cifuentes-Muñoz N, Márquez CL, Bulling M, Klingström J, Mancini R, Lozach P-Y,
640 Tischler ND. 2014. Hantavirus Gn and Gc glycoproteins self-assemble into virus-like particles. J
641 Virol 88:2344–2348.
642 20. Overby AK, Popov V, Neve EPA, Pettersson RF. 2006. Generation and analysis of infectious
643 virus-like particles of uukuniemi virus (bunyaviridae): a useful system for studying bunyaviral
644 packaging and budding. J Virol 80:10428–10435.

645 21. Acrani GO, Tilston-Lunel NL, Spiegel M, Weidmann M, Dilcher M, Andrade da Silva DE, Nunes
646 MRT, Elliott RM. 2015. Establishment of a minigenome system for Oropouche virus reveals the
647 S genome segment to be significantly longer than reported previously. J Gen Virol 96:513–523.
648 22. Kohl A, Hart TJ, Noonan C, Royall E, Roberts LO, Elliott RM. 2004. A bunyamwera virus
649 minireplicon system in mosquito cells. J Virol 78:5679–5685.
650 23. Tilston-Lunel NL, Shi X, Elliott RM, Acrani GO. 2017. The Potential for Reassortment between
651 Oropouche and Schmallenberg Orthobunyaviruses. Viruses 9:E220.
652 24. Elliott RM, Blakqori G, van Knippenberg IC, Koudriakova E, Li P, McLees A, Shi X, Szemiel AM.
653 2013. Establishment of a reverse genetics system for Schmallenberg virus, a newly emerged
654 orthobunyavirus in Europe. J Gen Virol 94:851–859.
655 25. Ogawa Y, Sugiura K, Kato K, Tohya Y, Akashi H. 2007. Rescue of Akabane virus (family
656 Bunyaviridae) entirely from cloned cDNAs by using RNA polymerase I. J Gen Virol 88:3385–3390.
657 26. Shi X, Kohl A, Léonard VHJ, Li P, McLees A, Elliott RM. 2006. Requirement of the N-terminal
658 region of orthobunyavirus nonstructural protein NSm for virus assembly and morphogenesis. J
659 Virol 80:8089–8099.
660 27. Klemm C, Reguera J, Cusack S, Zielecki F, Kochs G, Weber F. 2013. Systems to establish
661 bunyavirus genome replication in the absence of transcription. J Virol 87:8205–8212.
662 28. Tilston-Lunel NL, Acrani GO, Randall RE, Elliott RM. 2015. Generation of Recombinant
663 Oropouche Viruses Lacking the Nonstructural Protein NSm or NSs. J Virol 90:2616–2627.
664 29. Shi X, Botting CH, Li P, Niglas M, Brennan B, Shirran SL, Szemiel AM, Elliott RM. 2016.
665 Bunyamwera orthobunyavirus glycoprotein precursor is processed by cellular signal peptidase
666 and signal peptide peptidase. Proc Natl Acad Sci U S A 113:8825–8830.
667 30. Hellert J, Aebischer A, Wernike K, Haouz A, Brocchi E, Reiche S, Guardado-Calvo P, Beer M,
668 Rey FA. 2019. Orthobunyavirus spike architecture and recognition by neutralizing antibodies. Nat
669 Commun 10:879.
670 31. Krogh A, Larsson B, von Heijne G, Sonnhammer EL. 2001. Predicting transmembrane protein
671 topology with a hidden Markov model: application to complete genomes. J Mol Biol 305:567–580.
672 32. Nielsen H. 2017. Predicting Secretory Proteins with SignalP. Methods Mol Biol 1611:59–73.
673 33. Fujiwara T, Oda K, Yokota S, Takatsuki A, Ikehara Y. 1988. Brefeldin A causes disassembly of
674 the Golgi complex and accumulation of secretory proteins in the endoplasmic reticulum. J Biol
675 Chem 263:18545–18552.
676 34. Mollenhauer HH, Morré DJ, Rowe LD. 1990. Alteration of intracellular traffic by monensin;
677 mechanism, specificity and relationship to toxicity. Biochim Biophys Acta 1031:225–246.
678 35. Sciaky N, Presley J, Smith C, Zaal KJ, Cole N, Moreira JE, Terasaki M, Siggia E, Lippincott-
679 Schwartz J. 1997. Golgi tubule traffic and the effects of brefeldin A visualized in living cells. J Cell
680 Biol 139:1137–1155.
681 36. Crump CM, Yates C, Minson T. 2007. Herpes simplex virus type 1 cytoplasmic envelopment
682 requires functional Vps4. J Virol 81:7380–7387.
683 37. Zamborlini A, Usami Y, Radoshitzky SR, Popova E, Palu G, Göttlinger H. 2006. Release of
684 autoinhibition converts ESCRT-III components into potent inhibitors of HIV-1 budding. Proc Natl
685 Acad Sci U S A 103:19140–19145.
686 38. Pawliczek T, Crump CM. 2009. Herpes simplex virus type 1 production requires a functional
687 ESCRT-III complex but is independent of TSG101 and ALIX expression. J Virol 83:11254–11264.
688 39. Shi X, Lappin DF, Elliott RM. 2004. Mapping the Golgi targeting and retention signal of
689 Bunyamwera virus glycoproteins. J Virol 78:10793–10802.
690 40. Overby AK, Pettersson RF, Neve EPA. 2007. The glycoprotein cytoplasmic tail of Uukuniemi virus
691 (Bunyaviridae) interacts with ribonucleoproteins and is critical for genome packaging. J Virol
692 81:3198–3205.
693 41. Shi X, Kohl A, Li P, Elliott RM. 2007. Role of the cytoplasmic tail domains of Bunyamwera
694 orthobunyavirus glycoproteins Gn and Gc in virus assembly and morphogenesis. J Virol
695 81:10151–10160.
696 42. Shi X, Brauburger K, Elliott RM. 2005. Role of N-linked glycans on bunyamwera virus
697 glycoproteins in intracellular trafficking, protein folding, and virus infectivity. J Virol 79:13725–
698 13734.
699 43. Kaufman RJ. 1999. Stress signaling from the lumen of the endoplasmic reticulum: coordination of
700 gene transcriptional and translational controls. Genes Dev 13:1211–1233.

701 44. Novoa RR, Calderita G, Cabezas P, Elliott RM, Risco C. 2005. Key Golgi factors for structural
702 and functional maturation of bunyamwera virus. J Virol 79:10852–10863.
703 45. Butt BG, Owen DJ, Jeffries CM, Ivanova L, Hill CH, Houghton JW, Ahmed MF, Antrobus R,
704 Svergun DI, Welch JJ, Crump CM, Graham SC. 2020. Insights into herpesvirus assembly from
705 the structure of the pUL7:pUL51 complex. Elife 9:e53789.
706 46. Streck NT, Carmichael J, Buchkovich NJ. 2018. Nonenvelopment Role for the ESCRT-III Complex
707 during Human Cytomegalovirus Infection. J Virol 92:e02096-17.
708 47. Kilmartin JV, Wright B, Milstein C. 1982. Rat monoclonal antitubulin antibodies derived by using
709 a new nonsecreting rat cell line. J Cell Biol 93:576–582.
710 48. Schindelin J, Arganda-Carreras I, Frise E, Kaynig V, Longair M, Pietzsch T, Preibisch S, Rueden
711 C, Saalfeld S, Schmid B, Tinevez J-Y, White DJ, Hartenstein V, Eliceiri K, Tomancak P, Cardona
712 A. 2012. Fiji: an open-source platform for biological-image analysis. Nat Methods 9:676–682.
713 49. Rueden CT, Schindelin J, Hiner MC, DeZonia BE, Walter AE, Arena ET, Eliceiri KW. 2017.
714 ImageJ2: ImageJ for the next generation of scientific image data. BMC Bioinformatics 18:529.
715